Bone regeneration using 3D-printed polycaprolactone scaffold mixed with β-tricalcium phosphate in rabbit calvarial defects

Hyung-Chul Pae

Department of Dentistry
The Graduate School, Yonsei University

Bone regeneration using 3D-printed polycaprolactone scaffold mixed with β-tricalcium phosphate in rabbit calvarial defects

Directed by Professor Seong-Ho Choi

The Doctoral Dissertation
submitted to the Department of Dentistry
and the Graduate School of Yonsei University
in partial fulfillment of the requirements for the degree of
Ph.D. in Dental Science

Hyung-Chul Pae

This certifies that the Doctoral Dissertation
of Hyung-Chul Pae is approved.

Thesis Supervisor: Seong-Ho Choi

Ui-Won Jung

Jung-Seok Lee

Jeong-Won Paik

Jae-Kook Cha

The Graduate School
Yonsei University
December 2020

감사의 글

치주를 공부하게 되어 많은 것이 낯설고 어렵던 적이 엊그제 같은데 지금은 학위논문이 완성되어 박사학위를 받게 되었다는 사실이 매우 뿌듯합니다. 그 배움의 과정에서 도와주신 많은 분들께 진심으로 감사의 인사를 드립니다.

항상 넓은 아량으로 제자들을 이끌어주시고 많은 것들을 베풀어주시는 최성호 교수님께 감사드립니다. 항상 저를 믿어주시고 예뻐해 주셨기에 제가 제 능력 이상의 것들을 펼칠 수 있었고 미숙한 제가 지금에 이를 수 있었던 것 같습니다. 인생에서 최성호 교수님을 스승으로 만났다는 사실에 항상 감사하며 지낼 것 같습니다. 아울러 치주과 의사로 성장하기까지 임상과 학문에 대한 가르침을 주신 채중규 교수님, 조규성 교수님, 김창성 교수님, 정의원 교수님, 이중석 교수님, 차재국 교수님, 백정원 교수님께도 깊은 감사의 말씀을 드립니다. 훌륭한 임상가이자 연구자인 연세대학교 치주과 교수님들 곁에서 그동안 많은 것들을 배울 수 있어 영광이었습니다. 학위 과정과 의국 생활에서 동고동락을 같이 한 치주과 동기들과 의국 선후배 선생님들에게도 고마운 마음을 전합니다. 특히, 1년차 시절 아무것도 모르는 저에게 많은 임상적 가르침을 준 진영이 형, 항상 웃음과 지지와 사랑을 보내주는 주현 누나, 궂은 일, 사소한 일, 어려운 일 가리지 않고 믿음직하게 처리해주는 인표에게 많이 감

사합니다.

마지막으로, 제 옆에서 버팀목이 되어주고 있는 가족들에게도 감사하다는 말을 전합니다. 뒤에서 말없이 항상 응원해주시고 그 자체만으로도 제게 힘이 되어 주시는 부모님께 사랑한다는 말을 전합니다. 코로나 때문에 오랫동안 만나지도 못하고 외국에 있는 두 형들에게도 감사하고 보고싶다는 말을 전합니다. 또한 저를 항상 아들처럼 챙겨주시는 장인어른과 장모님께 감사드리며, 마지막으로 제 바로 옆에서 즐거울 때에는 사랑을 주고 힘들거나 걱정이 있을 때에는 든든한 격려와 믿음을 주는 아내 예준이와 아들 민우에게 사랑하고 감사하다는 말을 하고 싶습니다.

2020년 12월

배 형 철

Table of Contents

List of Figures ····· ii
List of Table ····· iii
Abstract (English) ····· iv
I. Introduction ····· 1
II. Materials & Methods ····· 4
1. Materials ····· 4
2. Study design ····· 6
3. Surgical procedures ····· 6
4. Evaluation methods ····· 7
III. Results ····· 11
1. Mechanical testing of PCL and PCL/β-TCP 3D block ····· 11
2. Clinical observations ····· 11
3. Micro CT analysis ····· 11
4. Histologic findings ····· 12
5. Histomorphometric analysis ····· 13
IV. Discussion ····· 15
V. Conclusion ····· 20
References ····· 21
Figures ····· 26
Tables ····· 33
Abstract (Korean) ····· 35

List of Figures

Figure 1. Schematic diagram of the 3D bio-printing system (A) and 3D polycaprolactone scaffold (B) ····· 26

Figure 2. Strut and pore sizes of 3D scaffolds ····· 27

Figure 3. Surgical procedure ····· 28

Figure 4. 3D reconstructed micro-CT images of defects at 2 and 8 weeks ····· 29

Figure 5. Histologic images after 2 weeks ····· 30

Figure 6. Histologic images after 8 weeks ····· 31

Figure 7. New bone formation around PCL/β-TCP scaffold ····· 32

List of Tables

Table 1. Total augmented volume and new bone volume measured with micro-CT grey value ····· 33

Table 2. Total augmented area, new bone area and residual material area (histomorphometric analysis) ····· 34

Abstract

Bone regeneration using 3D-printed polycaprolactone scaffold mixed with β-tricalcium phosphate in rabbit calvarial defects

Hyung-Chul Pae, D.D.S;

Department of Dentistry
The Graduate School, Yonsei University

(Directed by Professor Seong-Ho Choi, D.D.S., M.S.D., PhD.)

Background: Defect-specific bone regeneration using 3-dimensional (3D) printing of block bone has been developed. Polycaprolactone (PCL) is biocompatible polymer that can be used as 3D scaffold.

Purpose: The aim of this study is to assess osteogenic efficacy and biocompatibility of 3D printed PCL scaffold and to evaluate effectiveness of β-tricalcium phosphate (β-TCP) addition in PCL scaffold.

Materials and methods: Four circular defects (diameter: 8mm) in rabbit calvarium were randomly assigned to i) negative control (control), ii) PCL block (PCL), iii)

PCL mixed with 10 wt% β-TCP (PCL/β-TCP), and iv) PCL/β-TCP plus collagen membrane (PCL/β-TCP+M). Animals were euthanized at 2 (*n=5*) and 8 weeks (*n=5*). Outcome measures included micro-computed tomography (CT) and histomorphometric analysis.

Results: In micro-CT, PCL/β-TCP+M showed the highest total augmented volume and new bone volume at 8 weeks, but there was no significant difference among four groups. Histomorphometrically, PCL, PCL/β-TCP, PCL/β-TCP+M showed the significantly higher total augmented area compared to the control. PCL/β-TCP+M showed the highest new bone area, but not statistically higher than the control. New bone formation deep inside the scaffold was observed only in β-TCP added scaffold.

Conclusion: PCL showed high biocompatibility with great volume maintenance. Addition of β-TCP to PCL seemed to increase hydrophilicity and osteoconductivity. Developments in 3D printed PCL material are expected.

Key words: bone regeneration, beta tricalcium phosphate, polycaprolactone, 3D printing

Bone regeneration using 3D-printed polycaprolactone scaffold mixed with β-tricalcium phosphate in rabbit calvarial defects

Hyung-Chul Pae, D.D.S;

Department of Dentistry
The Graduate School, Yonsei University

(Directed by Professor Seong-Ho Choi, D.D.S., M.S.D., PhD.)

I. Introduction

As the implant dentistry has evolved, guided bone regeneration (GBR) became a predictable and routine protocol in the alveolar bone defects where implants are going to be placed[1]. In particular, GBR is essential for restoration-driven positioning and esthetics of implants in atrophied alveolar ridge[2]. Furthermore, various materials, timing, and methods of GBR are being considered and developing for high osteogenesis and easy manipulation.

Generally, GBR with particulated bone substitute and collagen membrane can be

performed regardless of defect size and shape. However, it is vulnerable to external force, so it can be easily collapsed with low stability[3,4]. As an alternative to this, block type bone substitute can be used with higher space-maintaining ability and better stability at the defect site[5,6]. Nevertheless, the disadvantage of such a block-type bone substitute is that it is difficult to obtain a desired shape suitable for a defect, and the available amount of commonly used autogenous or allogenous block bone is also limited[7].

To overcome this problem, various techniques such as 3-dimensional (3D) printing and computer-aided design and computer-aided manufacturing (CAD-CAM) of block bone have been developed in the periodontal and bone regeneration area so that patient and defect-specific GBR procedures can be performed. By using the prepared block bone made from the CT images of patient's defects, the operation time and difficulty can be reduced with favorable clinical outcomes[8,9].

Many materials that can be used as 3D scaffolds in the fields of tissue engineering and medical engineering have been developed, including bioresorbable polymers such as polycaprolactone (PCL) which have shown biocompatible results[10,11]. 3D printed PCL has been used for a variety of purposes ranging from long term contraceptive devices in the medical field to bone fillers in cranial defects[10]. These biodegradable polymeric bone substitutes are also useful in situations where it is necessary to maintain volume in the extraction socket as in extraction socket preservation, showing high mechanical strength and slow degradation rate. In previous in-vivo study, 3D PCL scaffolds in human fresh extraction sockets showed normal bone healing and maintained the ridge height higher than

that in control group[12].

Nevertheless, PCL being a hydrophobic polymer, it is difficult for blood to infiltrate deep into the scaffold and it does not have a degradation rate that matches the rate of new bone formation. One of the ways to overcome these problems is to add ceramics such as β-tricalcium phosphate (β-TCP) to the PCL to increase hydrophilicity, osteoconductivity and the degradation rate to promote bone formation[10]. Many previous studies showed that the ceramic addition to these polymers enhanced the bone formation as well as the adhesion and proliferation of pre-osteoblast cells[13-16].

In general, when using a membrane in the GBR procedure, it prevents the penetration of overlying soft connective tissue and keeps the shape of downward particulated bone substitutes with volume maintenance[17]. On the other hand, the effect of using membranes in block bone grafts is not clear yet. In the block bone, membranes can be used to prevent the penetration of overlying soft connective tissue and rapid degradation of bone substitutes rather than to maintain its volume.

To keep pace with these patient-specific treatments, we are looking for materials that can be made into desired shape using 3D printing technology. There are many in-vitro experiments regarding 3D-printed PCL scaffolds, but there is little in-vivo study yet. Therefore, our first objective of this study was to assess the osteogenic efficacy and biocompatibility of 3D printed PCL scaffold and PCL scaffold mixed with β-TCP for bone regeneration, and second objective was to evaluate effectiveness of β-TCP addition in PCL scaffold.

II. Materials and methods

1. Materials

PCL (Polycaprolactone) and PCL/β-TCP 3D block

PCL (average molecular weight = 45,000 g/mol) and β-TCP were purchased from Polysciences and Sigma Aldrich. The 3D PCL and PCL/β-TCP scaffolds were prepared by 3D printing (3D Bio Printer, M4T-100, M4T Co. Ltd., Korea), as shown in Figure 1A. PCL pellets were melted at 100℃ in a heating cylinder and 10 wt% β-TCP was added. PCL and PCL/β-TCP mixtures were ejected through a heated nozzle of compressed dry air at a pressure of 300 kPa and the feed rate was set to 50 mm/min. The scaffold struts could be plotted as layer-by-layer deposition on a stage. The 3D scaffolds (strut size = 520 ~ 540 μm and pore size = 240 ~ 260 μm) were fabricated into discs (diameter= 8 mm and height= 1.9 mm, Figure 1B, 2).

Mechanical testing of PCL and PCL/β-TCP 3D block

With reference to previously published studies[18-20], the compressive strength of the scaffolds was measured. Six samples (diameter= 8 mm and height= 1.9 mm) of each scaffold were tested on Universal testing machine (3366, Instron® Co.Ltd, Norwood, MA, USA) and 10 kN load cell. The samples were compressed at a speed of 1 mm/min until a strain level of approximately 75%. With recorded data regarding the load (kN) and deformation (mm), stress-strain curves of each sample were drawn. With the exception of

the first toe region caused by the initial settling of the sample, Young's modulus (stiffness) was calculated from the slope of the initial linear portion of the stress-strain curve, and compressive strength at yield was calculated from the intersection of the stress–strain curve and the line with modulus slope at an offset of 1.0% strain.

Collagen membrane

The bilayered chemically cross-linked type-I collagen membrane (CCM) (Rapigide II, Dalim Tissen co., Ltd., Seoul, Korea) was used in this study. It is derived from porcine skin and composed of type I collagen. The membrane has two layers, a compact non-porous film layer facing the soft connective tissue and a porous sponge layer facing the bone defect.

Animals

Ten male New Zealand White rabbits (body weight, 2.8-3.2 kg) were used in this experiment. All rabbits were housed in different cages with standard laboratory conditions and standard laboratory diet. All the procedures from animal selection, care, and preparation to anesthesia and surgical steps followed protocols approved by the Institutional Animal Care and Use Committee (Yonsei Medical Center, Seoul, Korea; approval number 2017-0117). All the protocols followed the ARRIVE (Animal Research: Reporting of *In Vivo* Experiments) guidelines for the study design[21].

2. Study design

Four round defects with 8 mm in diameter were created in each rabbit calvarium. The defects on the calvarium were randomly assigned to one of the following four treatment groups.

- Control group: filled with blood clot only
- PCL group: PCL block
- PCL/β-TCP group: PCL block with 10 wt% β-TCP
- PCL/β-TCP + M group: PCL block with 10 wt% β-TCP plus cross-linked collagen membrane

The animals were euthanized at 2 weeks (n = 5) or 8 weeks (n = 5) after surgical procedure and specimens were harvested.

3. Surgical procedures

The previously published study was referred to for the surgical procedures[22]. General anesthesia was performed with alfaxan (5mg/kg, subcutaneous injection) and isoflurane (2-2.5%, inhalation). After disinfection with povidone iodine and local anesthesia with 2% lidocaine, an incision was made along the midline of the cranium with 2cm long. A full-thickness flap was elevated and the calvarium was exposed. Under saline irrigation, four round defects with 8 mm in diameter each were created with a trephine bur without damaging underlying dura mater and brain tissue. The defects on the calvarium were randomly assigned to one of the following four treatment groups; Control group, PCL

group, PCL/β-TCP group, and PCL/β-TCP+M group (Figure 3).

In group PCL/β-TCP + M, the bone substitute block made of PCL with 10 wt% β-TCP was placed into the defect, followed by covering the entire site with the membrane cut into the size of 10 x 10 mm. The membrane was hydrated and applied without suture or tissue adhesive. The hydrated collagen membrane itself was immobilized because it had some adhesion to the bone tissue and PCL material. In group PCL/ β-TCP, only the bone substitute block made of PCL with 10 wt% β-TCP was placed into the defect. In group PCL, only the PCL block was inserted into the defect in the same manner. The prepared blocks were fabricated with 3D printing to match the 8mm defect diameter made with the trephine bur. The fit and movement of scaffolds were checked after application to the defect. In control, the defect was filled with the blood clot only. PCL and PCL/β-TCP blocks were immersed in 70% alcohol for 20 minutes, rinsed with saline, and then dried before being placed in the defect. After insertion of materials, the flaps were repositioned carefully and sutured with the absorbable 4-0 suture material (Vicryl, Ethicon, Somerville, NJ, USA).

4. Evaluation methods

Clinical observations

Animals were carefully observed and evaluated for complications such as inflammation, allergic reaction, post-operative bleeding and infection around the surgical site for 2 and 8 weeks after surgery.

Micro-CT analysis

The harvested specimens were fixed with 10% formalin and then scanned with a micro-computed tomography (Sky-Scan 1173, SkyScan, Kontich, Belgium) at a resolution of 13.85 μm (130 kV, 60 μA). The scanned data sets were processed in DICOM (Digital Imaging and Communications in Medicine) format, and the region of interest (ROI) was reconstructed with 3-dimensional (3D) reconstruction software (Nrecon reconstruction program, SkyScan, Kontich, Belgium). The lateral boundary of the ROI was the initial defect margin made by the trephine bur, superior boundary was soft connective tissue border, and inferior boundary was dura mater. The total volume of the ROI was set as the total augmented volume and the new bone volume was measured from new bone in the ROI. Radiopaque areas were distinguished from the radiolucent fibrovascular connective tissue with 8-bit threshold grayscale values. The gray-scale values were set from 68 to 255 for newly formed bone in the defects. The volume of voxels with the grayscale values in this range was taken as the volume of the newly formed bone. Areas with grayscale values lower than 68 were considered as fibrovascular connective tissue. This threshold was selected by an experienced operator according to specimen-specific thresholds[23,24]. The volume of each grayscale value range was calculated with the 3D reconstruction software. PCL blocks were not distinguished from fibrovascular connective tissue, so these areas could not be measured by the micro-CT. Within the ROI, the following parameters were measured.

- Total augmented volume (TAV; mm^3): total augmented volumes

- New bone volume (NBV; mm^3): volumetric measurements of the newly formed bone within the defects

Histologic and histomorphometric analysis

After fixed in 10% formalin, the specimens were decalcified in 5% formic acid for 14 days and then embedded in paraffin. 5μm-thick serial sections were obtained through the middle portion of each circular defect. The sections were stained with hematoxylin-eosin and Masson trichrome. The stained histologic slides were examined with a light microscope (DM LB, Leica Microsystems, Wetzlar, Germany) equipped with a camera (DC300F, Leica Microsystems, Wetzlar, Germany). After the microscopic examination assessing overall status of various tissues, the slide images were digitally captured and computer-aided histometric measurements of defects were performed using an automated image analysis program (CaseViewer 2.1; 3DHISTECH ltd., Budapest, HUNGARY) and a computer software (Photoshop® CS6, Adobe System, San José, CA, USA). The lateral boundary of the ROI was the initial round defect margin formed by the trephine bur, superior boundary was collagen membrane or soft connective tissue border, and inferior boundary was dura mater. The total area of the ROI was set as the total augmented area, and the new bone area and residual material area was measured from new bone and residual material in the ROI. Those areas of the new bone and residual material in the ROI are visually bounded, and then automatically calculated using functions of the programs. Within the ROI, the following parameters were measured.

- Total augmented area (TAA; mm^2): The sum area of new bone, block bone substitute, and fibrovascular connective tissue within the ROI
- New bone area (NBA; mm^2): Area of new bone within the ROI.
- Residual material area (RMA; mm^2): Area of the residual graft material within the ROI.

Statistical analysis

The statistical analysis was conducted using commercially available SPSS software program (IBM SPSS Statistics 23, SPSS, Chicago, IL). Mann-Whitney-U test was used to analyze the differences of stiffness and compressive strength between two scaffolds. Measurements from micro-CT volume and histologic area were summarized regarding the mean values and standard deviations (SD). Kruskal-Wallis test and Mann-Whitney-U test (nonparametric analysis) was used to analyze the difference among the four groups at each time period and between the same groups of two healing periods. Statistical significance was considered when $P<0.05$.

III. Results

1. Mechanical testing of PCL and PCL/β-TCP 3D block

Compressive strength of PCL and PCL/β-TCP 3D block was measured. Stiffness of PCL scaffold (46.7±1.7 N/mm) was statistically higher than PCL/β-TCP scaffold (35.7±3.1 N/mm) (P=0.002). Compressive yield strength of PCL (56.9±2.3 MPa) was statistically higher than PCL/β-TCP (46.2±3.1 MPa) (P=0.002).

2. Clinical observations

There was no severe postoperative complication such as bleeding and swelling. Surgical sites of rabbits were healed well without infection or flap exposure. All animals had no specific event during experimental period.

3. Micro CT analysis

The results of the micro CT analysis are summarized in Table 1. In the 3D reconstructed view, the new bone was hardly formed in the inner part of the PCL block but mainly formed around the PCL block (Figure 4).

At 2 weeks, the PCL/β-TCP group showed the highest TAV (217.06±28.82 mm^3), and there was significant difference compared to controls (P=0.032) but not compared to the other groups. The PCL/β-TCP group also demonstrated the highest NBV (18.25±5.45 mm^3), but there was no significant difference among four groups at 2 weeks regarding NBV.

At 8 weeks, PCL/β-TCP+M group showed the highest TAV (216.25±25.66) and NBV (35.34±10.92), but there was no significant difference among four groups at 8 weeks regarding TAV and NBV.

4. Histologic findings

Control group

At 2 weeks, new bone formation was observed from the periphery (Figure 5A). The defect spaces were collapsed by soft tissues. At 8 weeks, more mature bone formation was observed further into the center of the defect (Figure 6A).

PCL group

At 2 weeks, defect space was well maintained by PCL scaffold with new bone formation from the periphery (Figure 5B). At 8 weeks, PCL scaffold also occupied the defect space without distinct degradation. In the middle of defect below the PCL scaffold, new bone formation could be observed (Figure 6B). The new bone seemed to hardly grow inside the PCL scaffold.

PCL/β-TCP group

At 2 weeks, defect space was also well maintained by PCL/β-TCP scaffold (Figure 5C). At 8 weeks, new bone formation could be observed from the periphery of defect and above the PCL/β-TCP scaffold (Figure 6C). Only 2 specimens in 2 weeks showed new bone

formation inside the scaffold. The PCL blocks were hardly degraded and maintained the original structures.

PCL/β-TCP + M group

At 2 weeks, the collagen membrane was well positioned between overlying soft tissues and PCL/β-TCP scaffold. The new bone formation was also mainly on the periphery of defect (Figure 5D). At 8 weeks, the collagen membrane showed some resorption compared to 2 weeks. The new bone was well formed below and above the PCL/β-TCP scaffold from the periphery (Figure 6D). In 4 out of 5 specimens at 8 weeks, new bone was observed inside the scaffold.

5. Histomorphometric analysis

The results from the histomorphometric analysis are summarized in Table 2.

2 weeks

At 2 weeks, the PCL/β-TCP+M group (14.31±2.04 mm^2) showed the highest TAA. PCL (13.96±1.52 mm^2), PCL/β-TCP (13.11±1.33 mm^2), PCL/β-TCP+M groups showed the significantly higher TAA when compared to the control (6.39±1.50 mm^2) (P=0.008, 0.008, 0.008 respectively).

Regarding NBA at 2 weeks, the control group (1.52±0.57 mm^2) revealed the highest NBA, but there was no significant difference among four groups.

8 weeks

At 8 weeks, the PCL group (14.93±3.26 mm^2) showed the highest TAA. The PCL, PCL/β-TCP (10.93±1.84 mm^2), PCL/β-TCP+M (11.59±0.79 mm^2) groups showed the significantly higher TAA when compared to the control (6.24±1.71 mm^2) (*P*=0.008, 0.016, 0.008 respectively). Nevertheless, among PCL, PCL/β-TCP, PCL/β-TCP+M group, there was no statistically significant difference.

In regards to the NBA, PCL/β-TCP+M (2.66±0.91 mm^2) showed the highest NBA, but not statistically higher than the control (2.63±0.95 mm^2), PCL (1.61±1.03 mm^2), and PCL/β-TCP (1.20±0.62 mm^2) group (*P*=1.000, 0.222, 0.056 respectively).

Between 2 & 8 weeks

In 4 groups, there was no statistically significant difference regarding TAA between 2 and 8 weeks (control: *P*=1.000, PCL: *P*=0.690, PCL/β-TCP: *P*=0.056, PCL/β-TCP+M: *P*=0.056). In regards to NBA, PCL/β-TCP plus membrane groups between 2 and 8 weeks showed the statistically significant difference (*P*=0.032). Whereas, in the control, PCL, and PCL/β-TCP groups, significant difference of new bone formation was not found (*P*=0.056, 0.222, 0.548 respectively).

IV. Discussion

In this study, a 3D printed PCL scaffold was used and evaluated for its usage in GBR. PCL is a polymer which is hardly degraded and shows good results in maintaining volume regardless of whether or not a membrane was used. Generally, when using only bone graft material without a membrane, soft connective tissue tends to infiltrate through the bone graft material[25,26]. However, in this experiment, the upper soft connective tissue did not penetrate into the scaffold even though a membrane was not used. Furthermore, some specimens rather showed a tendency of new bone formation between the upper soft tissue and the scaffold (Figure 6C, D).

In micro-CT, it was difficult to observe and evaluate PCL blocks. The gray value of PCL was similar to surrounding soft tissues and could not be distinguished radiographically. However, in the block with β-TCP, the approximate scaffold shape was distinguished by small dots representing β-TCP, but it was also impossible to quantitatively analyze its volume.

Histomorphometrically, it showed no specific inflammatory reaction around the PCL block with or without 10 wt% β-TCP. PCL, a biocompatible polymer, is known as a safe material in many other studies[14,27,28], and this study also showed biocompatibility of this material in the rabbit in vivo. When pure PCL or PCL mixed with β-TCP were used, there was less new bone formation than the control group, but there was no statistically significant difference except PCL/β-TCP group at 8 weeks. The new bone was well formed around the PCL scaffold, but not inside the scaffold. Other in-vivo studies with histologic analysis

showed that the PCL scaffold was excellent in maintaining volume, but not in new bone formation, especially deep inside the scaffold[12,27,28]. In this study, two specimens of PCL/β-TCP group and four specimens of PCL/β-TCP with membrane group exhibited new bone formation up to deep inside of the scaffold, but direct bone contact was not observed in most specimens (Figure 7A). Bone substitutes without intimate bone contact are considered unfavorable with poor bone quality in the long-term[28,29]. However, in only one specimen of PCL/β-TCP with membrane group at 8 weeks, direct bone contact was observed between mature bone and the scaffold (Figure 7B). This inconsistency was also observed in the previous study using PCL scaffolds, showing high standard deviation regarding bone formation[30]. Because the research on PCL is still lacking, especially regarding characteristics such as optimal porosity or hydrophilicity for new bone growth, this material seems to still have such limitations. However, development of these characteristics is expected to make it possible to produce consistent results.

PCL is a polymer material that is stable in vivo but does not decompose well and is characterized by hydrophobicity. This hydrophobic nature might make it difficult for the osteogenic proteins and cells along with the blood to penetrate into the narrow pores (size = 240 ~ 260 μ) of the PCL scaffold. Therefore, in order to improve the hydrophobic properties of polymer, it could be mixed and coated with ceramic particles, or plasma treated on the surface[10,13,15]. In the previous in-vitro studies, the addition of magnesium oxide, hydroxyapatite or β-TCP followed by oxygen and nitrogen plasma treatment enhanced the adhesion, proliferation, and differentiation of pre-osteoblast cells in the PCL

scaffolds[13,14]. Surface morphology and chemical properties of the PCL scaffold could affect the pre-osteoblast cells[13,14]. In this study, pure PCL and PCL mixed with β-TCP were used. Compared with pure PCL, no statistically significant difference was observed in-vivo when β-TCP was added. However, only β-TCP mixed PCL group showed new bone deep inside the scaffold. It might be assumed that β-TCP mixed in PCL could induce hydrophilicity, osteoconductivity and cell affinity in some ways.

In this study, 3D printed PCL with strut size of 520 ~ 540 μm, pore size of 240 ~ 260 μm, block diameter of 8 mm, and block height of 1.9 mm was used. A 1.9 mm height block was created by layer-by-layer deposition using a nozzle of about 0.5 mm. Polymer scaffold should be structured considering both mechanical and biologic aspects. For the mechanical strength of the PCL scaffold, a certain level of strut size and pore size, the distance between struts, is required. Porosity, pore size, shape, structural connectivity is the main factors affecting mechanical properties in polymers[10,31,32]. According to the mechanical testing of this study, the scaffold seems to be able to withstand the forces that can be applied to the material during and after the surgery, although the compressive strength tended to decrease slightly with the addition of β-TCP. Biologically, the optimal pore size for osteoconduction is 200-350 μm considering that blood, proteins, and cells should penetrate into the hydrophobic polymer for new bone formation by the previous studies[33,34]. On the other hand, in another in-vivo study using beagle dogs, the PCL of 1200 μm pore size showed more new bone formation than the PCL of 400 μm pore size[28]. It seems that the PCL block used in this study was made to have an appropriate gap between struts in a layer, but the

space between each layer was almost none with struts of upper and lower layers stuck together as shown in Figures 5 and 6. Increasing the gap between each layer and reducing the thickness of the strut with more layers would have shown better results.

The diameter of the circular defect and scaffold was 8 mm, which is smaller than the critical size defect for observing early phase of bone regeneration and reducing individual variation demonstrated in the previous study[35]. However, the scaffold was not a perfect circle with irregular protrusion around the edge because it was made by turning each layer 45 degrees with a strut size of 520 ~ 540 μm. These irregular protrusions of incomplete circle caused poor fitting when the PCL scaffold was inserted into the 8mm cranial defect, even though it was easy to trim the block with metal instruments. Nonetheless, no soft connective tissue ingrowth was observed between the gap between the existing bone and the irregular scaffold. Instead, the new bone tended to fill the defect from these areas.

The PCL scaffold exhibited low osteoconductivity but great volume maintaining. The upper soft connective tissue did not infiltrate downwards in the groups with and without membrane. If the polymer is given a resilience that can be used as a membrane through tissue engineering process and 3D-printed as a defect-specific membrane, it may perform the function of space making frame with macro-porosity like titanium mesh[36,37]. The previous study compared PCL membrane with collagen membrane in beagle model[38]. In the in-vitro study which tested the mechanical stability and cell affinity of PCL membrane, this material showed good cell attachment and potential as a GBR membrane[39].

Material properties such as biodegradability, pore size, porosity, surface architecture and

mechanical property, which can change protein and cell infiltration and biocompatibility, are being developed with tissue engineering. As in this experiment, although PCL block still has limitations in terms of new bone formation, it is expected to improve the properties of PCL through adding other materials such as ceramics or various tissue engineering. Through these developments, PCL material could have ideal degradation rate that matches the rate of new bone formation with high hydrophilicity and proper mechanical properties.

V. Conclusion

According to this study, 3D printed β-TCP added PCL scaffold seems to be a biocompatible and favorable material to be used in GBR. Although more new bone formation was not observed in PCL or PCL/β-TCP block group than in control group, these polymer blocks showed high biocompatibility with great volume maintenance. Addition of β-TCP to PCL scaffold seemed to increase hydrophilicity and osteoconductivity. Developments in 3D printed PCL material with mechanical and chemical modification using various tissue engineering techniques are expected.

References

1. Klein MO, Grotz KA, Walter C, Wegener J, Wagner W, Al-Nawas B. Functional rehabilitation of mandibular continuity defects using autologous bone and dental implants - prognostic value of bone origin, radiation therapy and implant dimensions. Eur Surg Res 2009;43(3):269-275.
2. Retzepi M, Donos N. Guided Bone Regeneration: biological principle and therapeutic applications. Clin Oral Implants Res 2010;21(6):567-576.
3. Yang S, Lan L, Miron RJ, Wei L, Zhang M, Zhang Y. Variability in Particle Degradation of Four Commonly Employed Dental Bone Grafts. Clin Implant Dent Relat Res 2015;17(5):996-1003.
4. Park YH, Choi SH, Cho KS, Lee JS. Dimensional alterations following vertical ridge augmentation using collagen membrane and three types of bone grafting materials: A retrospective observational study. Clin Implant Dent Relat Res 2017;19(4):742-749.
5. Kim JW, Choi KH, Yun JH, Jung UW, Kim CS, Choi SH, Cho KS. Bone formation of block and particulated biphasic calcium phosphate lyophilized with Escherichia coli-derived recombinant human bone morphogenetic protein 2 in rat calvarial defects. Oral Surg Oral Med Oral Pathol Oral Radiol Endod 2011;112(3):298-306.
6. Hwang JW, Park JS, Lee JS, Jung UW, Kim CS, Cho KS, Lee YK, Choi SH. Comparative evaluation of three calcium phosphate synthetic block bone graft materials for bone regeneration in rabbit calvaria. J Biomed Mater Res B Appl Biomater 2012;100(8):2044-2052.
7. Lee JS, Lee JS, Kang MH, Jung UW, Choi SH, Cho KS. Proof-of-concept study of vertical augmentation using block-type allogenic bone grafts: A preclinical experimental study on rabbit calvaria. J Biomed Mater Res B Appl Biomater 2018.
8. Rasperini G, Pilipchuk SP, Flanagan CL, Park CH, Pagni G, Hollister SJ, Giannobile WV. 3D-printed Bioresorbable Scaffold for Periodontal Repair. J Dent

Res 2015;94(9 Suppl):153S-157S.

9. Yao Q, Wei B, Guo Y, Jin C, Du X, Yan C, Yan J, Hu W, Xu Y, Zhou Z, Wang Y, Wang L. Design, construction and mechanical testing of digital 3D anatomical data-based PCL-HA bone tissue engineering scaffold. J Mater Sci Mater Med 2015;26(1):5360.
10. Dhandayuthapani B, Yoshida Y, Maekawa T, Kumar DS. Polymeric Scaffolds in Tissue Engineering Application: A Review. International Journal of Polymer Science 2011.
11. Williams JM, Adewunmi A, Schek RM, Flanagan CL, Krebsbach PH, Feinberg SE, Hollister SJ, Das S. Bone tissue engineering using polycaprolactone scaffolds fabricated via selective laser sintering. Biomaterials 2005;26(23):4817-4827.
12. Goh BT, Teh LY, Tan DB, Zhang Z, Teoh SH. Novel 3D polycaprolactone scaffold for ridge preservation--a pilot randomised controlled clinical trial. Clin Oral Implants Res 2015;26(3):271-277.
13. Roh H-S, Jung S-C, Kook M-S, Kim B-H. In vitro study of 3D PLGA/n-HAp/β-TCP composite scaffolds with etched oxygen plasma surface modification in bone tissue engineering. Applied Surface Science 2016;388:321-330.
14. Roh HS, Lee CM, Hwang YH, Kook MS, Yang SW, Lee D, Kim BH. Addition of MgO nanoparticles and plasma surface treatment of three-dimensional printed polycaprolactone/hydroxyapatite scaffolds for improving bone regeneration. Mater Sci Eng C Mater Biol Appl 2017;74:525-535.
15. Gómez-Lizárraga K, Flores-Morales C, Del Prado-Audelo M, Álvarez-Pérez M, Piña-Barba M, Escobedo C. Polycaprolactone-and polycaprolactone/ceramic-based 3D-bioplotted porous scaffolds for bone regeneration: A comparative study. Materials Science and Engineering: C 2017;79:326-335.
16. Shim JH, Moon TS, Yun MJ, Jeon YC, Jeong CM, Cho DW, Huh JB. Stimulation of healing within a rabbit calvarial defect by a PCL/PLGA scaffold blended with TCP using solid freeform fabrication technology. J Mater Sci Mater Med

2012;23(12):2993-3002.

17. Park JY, Jung IH, Kim YK, Lim HC, Lee JS, Jung UW, Choi SH. Guided bone regeneration using 1-ethyl-3-(3-dimethylaminopropyl) carbodiimide (EDC)-cross-linked type-I collagen membrane with biphasic calcium phosphate at rabbit calvarial defects. Biomater Res 2015;19:15.
18. Hutmacher DW, Schantz T, Zein I, Ng KW, Teoh SH, Tan KC. Mechanical properties and cell cultural response of polycaprolactone scaffolds designed and fabricated via fused deposition modeling. Journal of Biomedical Materials Research: An Official Journal of The Society for Biomaterials, The Japanese Society for Biomaterials, and The Australian Society for Biomaterials and the Korean Society for Biomaterials 2001;55(2):203-216.
19. Zein I, Hutmacher DW, Tan KC, Teoh SH. Fused deposition modeling of novel scaffold architectures for tissue engineering applications. Biomaterials 2002;23(4):1169-1185.
20. Eshraghi S, Das S. Mechanical and microstructural properties of polycaprolactone scaffolds with one-dimensional, two-dimensional, and three-dimensional orthogonally oriented porous architectures produced by selective laser sintering. Acta biomaterialia 2010;6(7):2467-2476.
21. Kilkenny C, Browne WJ, Cuthill IC, Emerson M, Altman DG. Improving bioscience research reporting: the ARRIVE guidelines for reporting animal research. PLoS Biol 2010;8(6):e1000412.
22. Yang C, Unursaikhan O, Lee JS, Jung UW, Kim CS, Choi SH. Osteoconductivity and biodegradation of synthetic bone substitutes with different tricalcium phosphate contents in rabbits. J Biomed Mater Res B Appl Biomater 2014;102(1):80-88.
23. Bouxsein ML, Boyd SK, Christiansen BA, Guldberg RE, Jepsen KJ, Müller R. Guidelines for assessment of bone microstructure in rodents using micro–computed tomography. Journal of bone and mineral research 2010;25(7):1468-

1486.

24. Christiansen BA. Effect of micro-computed tomography voxel size and segmentation method on trabecular bone microstructure measures in mice. Bone reports 2016;5:136-140.
25. Jung UW, Lee JS, Lee G, Lee IK, Hwang JW, Kim MS, Choi SH, Chai JK. Role of collagen membrane in lateral onlay grafting with bovine hydroxyapatite incorporated with collagen matrix in dogs. J Periodontal Implant Sci 2013;43(2):64-71.
26. Yamada S, Shima N, Kitamura H, Sugito H. Effect of porous xenographic bone graft with collagen barrier membrane on periodontal regeneration. Int J Periodontics Restorative Dent 2002;22(4):389-397.
27. Goh BT, Chanchareonsook N, Tideman H, Teoh SH, Chow JK, Jansen JA. The use of a polycaprolactone-tricalcium phosphate scaffold for bone regeneration of tooth socket facial wall defects and simultaneous immediate dental implant placement in Macaca fascicularis. J Biomed Mater Res A 2014;102(5):1379-1388.
28. Park SA, Lee HJ, Kim KS, Lee SJ, Lee JT, Kim SY, Chang NH, Park SY. In Vivo Evaluation of 3D-Printed Polycaprolactone Scaffold Implantation Combined with beta-TCP Powder for Alveolar Bone Augmentation in a Beagle Defect Model. Materials (Basel) 2018;11(2).
29. Kohal RJ, Gubik S, Strohl C, Stampf S, Bachle M, Hurrle AA, Patzelt SB. Effect of two different healing times on the mineralization of newly formed bone using a bovine bone substitute in sinus floor augmentation: a randomized, controlled, clinical and histological investigation. J Clin Periodontol 2015;42(11):1052-1059.
30. Hwang K-S, Choi J-W, Kim J-H, Chung HY, Jin S, Shim J-H, Yun W-S, Jeong C-M, Huh J-B. Comparative Efficacies of Collagen-Based 3D Printed PCL/PLGA/β-TCP Composite Block Bone Grafts and Biphasic Calcium Phosphate Bone Substitute for Bone Regeneration. Materials 2017;10(4):421.
31. Anseth KS, Bowman CN, Brannon-Peppas L. Mechanical properties of hydrogels

and their experimental determination. Biomaterials 1996;17(17):1647-1657.

32. Nair LS, Laurencin CT. Biodegradable polymers as biomaterials. Progress in polymer science 2007;32(8-9):762-798.
33. y Leon CAL. New perspectives in mercury porosimetry. Advances in colloid and interface science 1998;76:341-372.
34. Whang K, Healy K, Elenz D, Nam E, Tsai D, Thomas C, Nuber G, Glorieux F, Travers R, Sprague S. Engineering bone regeneration with bioabsorbable scaffolds with novel microarchitecture. Tissue engineering 1999;5(1):35-51.
35. Sohn JY, Park JC, Um YJ, Jung UW, Kim CS, Cho KS, Choi SH. Spontaneous healing capacity of rabbit cranial defects of various sizes. J Periodontal Implant Sci 2010;40(4):180-187.
36. Rasia-dal Polo M, Poli PP, Rancitelli D, Beretta M, Maiorana C. Alveolar ridge reconstruction with titanium meshes: a systematic review of the literature. Med Oral Patol Oral Cir Bucal 2014;19(6):e639-646.
37. Sagheb K, Schiegnitz E, Moergel M, Walter C, Al-Nawas B, Wagner W. Clinical outcome of alveolar ridge augmentation with individualized CAD-CAM-produced titanium mesh. Int J Implant Dent 2017;3(1):36.
38. Won JY, Park CY, Bae JH, Ahn G, Kim C, Lim DH, Cho DW, Yun WS, Shim JH, Huh JB. Evaluation of 3D printed PCL/PLGA/beta-TCP versus collagen membranes for guided bone regeneration in a beagle implant model. Biomed Mater 2016;11(5):055013.
39. Fujihara K, Kotaki M, Ramakrishna S. Guided bone regeneration membrane made of polycaprolactone/calcium carbonate composite nano-fibers. Biomaterials 2005;26(19):4139-4147.

Figures

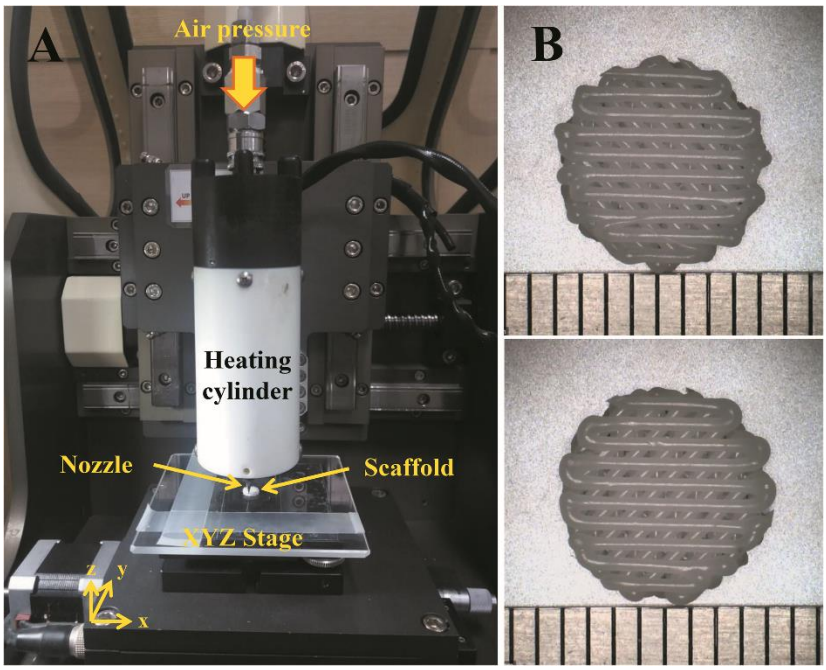

Figure 1. (A) Schematic diagram of the 3D bio-printing system (B) 3D polycaprolactone (up) and polycaprolactone/β-tricalcium phosphate (down) scaffolds

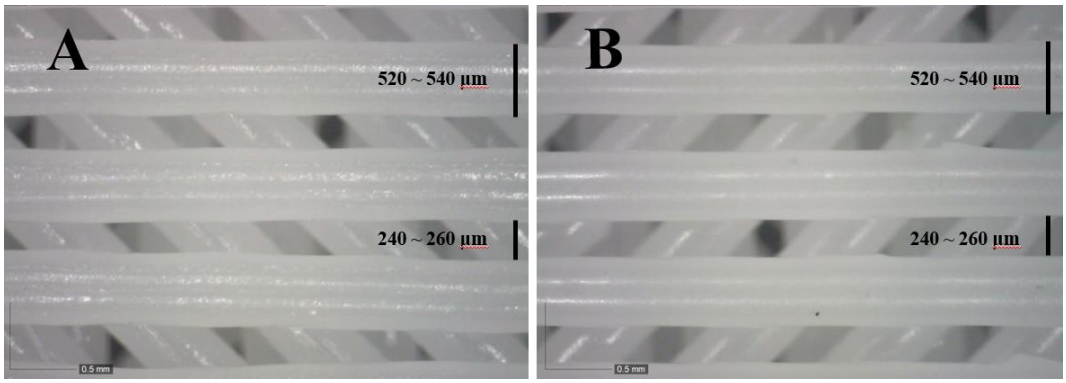

Figure 2. Strut and pore sizes of 3D polycaprolactone (A) and polycaprolactone/β-tricalcium phosphate (B) scaffolds (strut size = 520 ~ 540 μm, pore size = 240 ~ 260 μm)

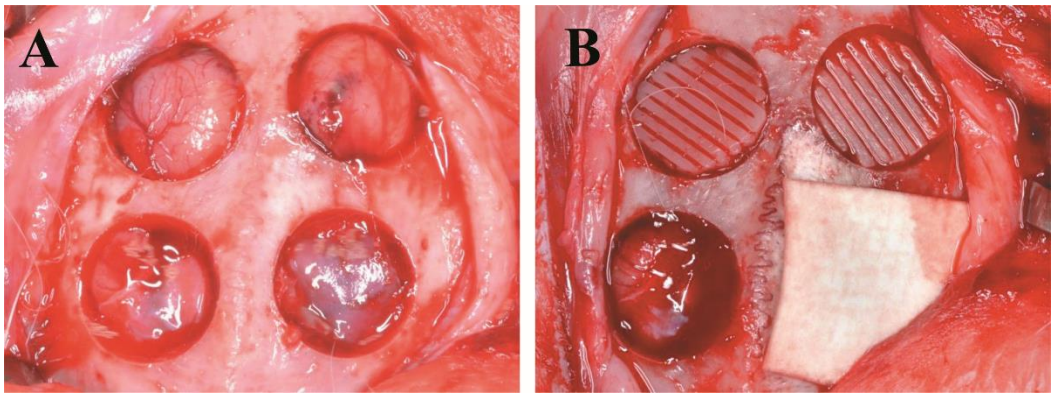

Figure 3. Surgical procedure (A) Four defects (ø=8mm) in the calvarium of 10 rabbits (B) Random assignment of defects, control group (left down), polycaprolactone group (left top), polycaprolactone/β-tricalcium phosphate group (right top), polycaprolactone/β-tricalcium phosphate plus collagen membrane group (right down)

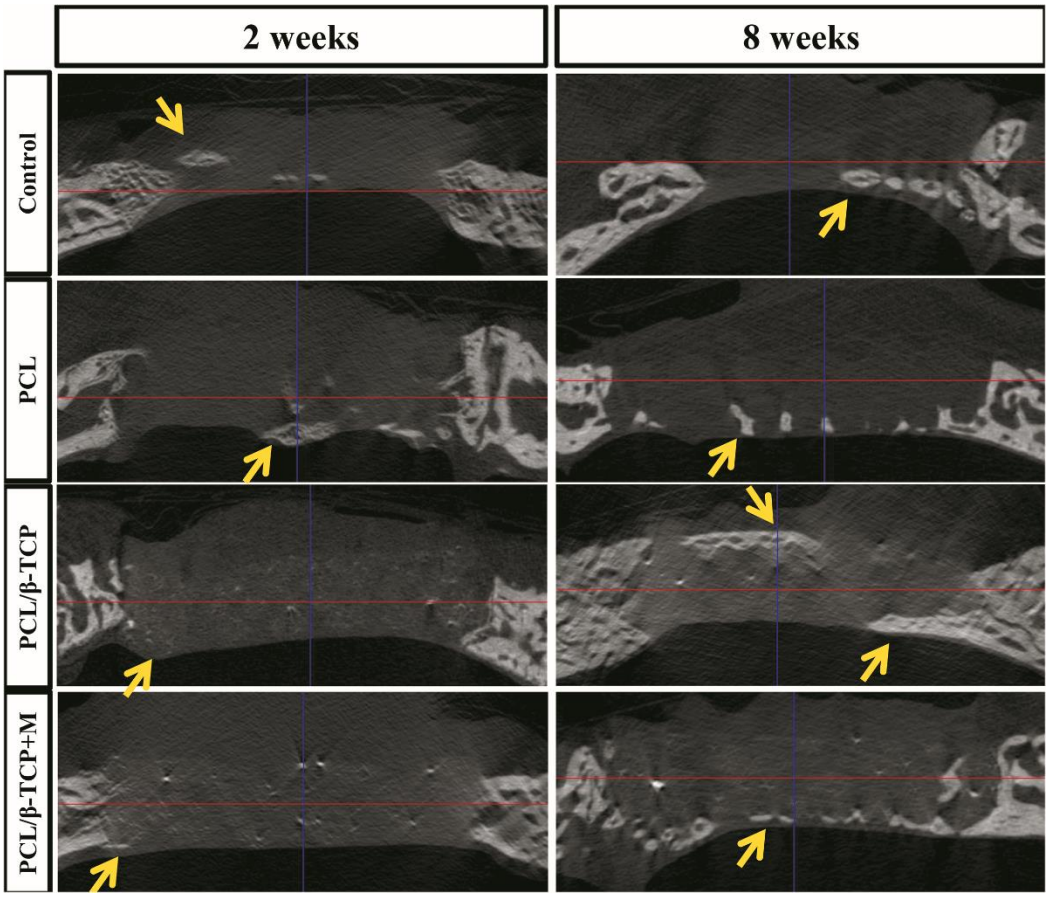

Figure 4. 3D reconstructed micro-CT images of defects at 2 and 8 weeks. New bone formation occurred mainly around the polycaprolactone scaffold, from the periphery of defect. (New bone formation is marked with arrows)

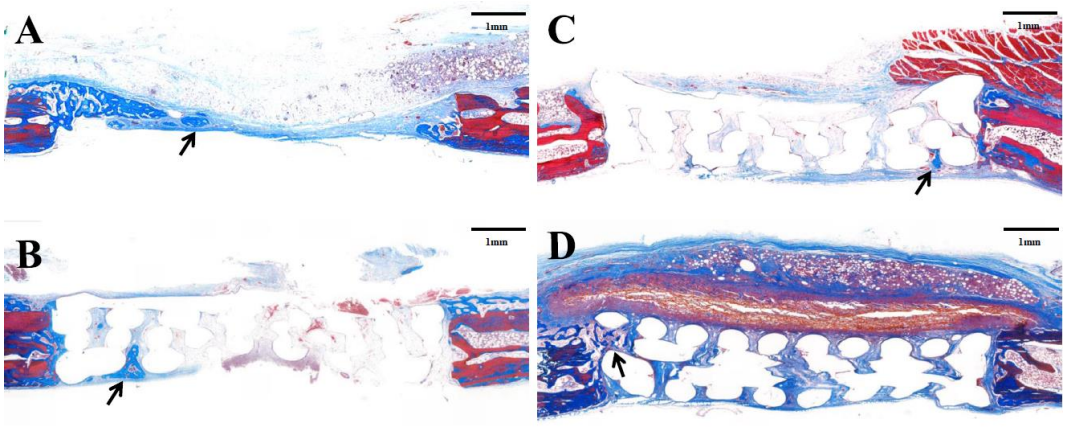

Figure 5. Histologic images after 2 weeks (Masson Trichrome, bar=1mm) (New bone formation is marked with arrows) (A) Control group; defect space is collapsed by overlying soft tissues. (B) PCL group; defect space is well maintained by PCL scaffold with new bone formation from the periphery. (C) PCL/β-TCP group; defect space is also well maintained by PCL/β-TCP scaffold. (D) PCL/β-TCP with membrane group; the collagen membrane is well positioned between overlying soft tissues and PCL/β-TCP scaffold. The new bone formation is also mainly on the periphery of defect.

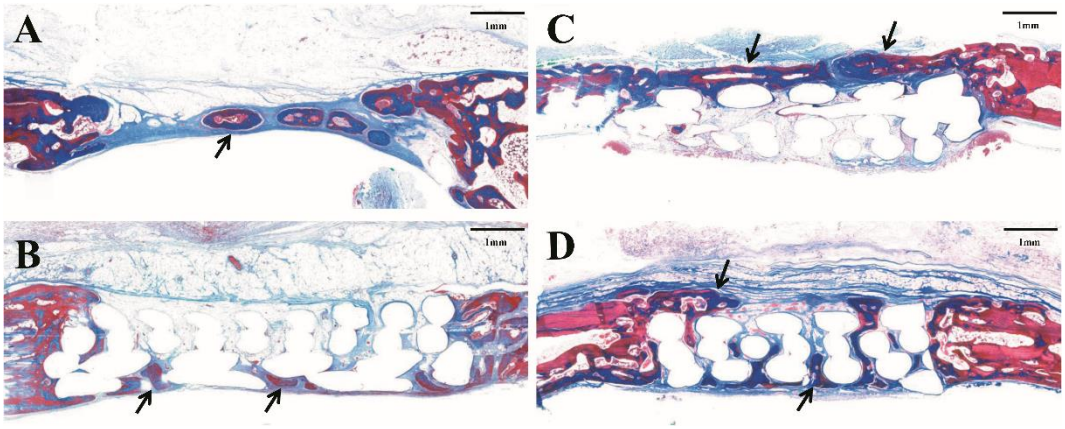

Figure 6. Histologic images after 8 weeks (Masson Trichrome, bar=1mm) (New bone formation is marked with arrows) (A) Control group; defect space is collapsed by overlying soft tissues with more mature bone formation compared to 2 weeks. (B) PCL group; PCL scaffold occupies the defect space without distinct resorption. In the middle of defect below the PCL scaffold, new bone formation can be observed. (C) PCL/β-TCP group; The marked new bone formation can be observed above the PCL/β-TCP scaffold, but not deep inside the scaffold. (D) PCL/β-TCP with membrane group; the collagen membrane shows some resorption compared to 2 weeks. The new bone is well formed inside and around the scaffold, but hardly contacting with the scaffold.

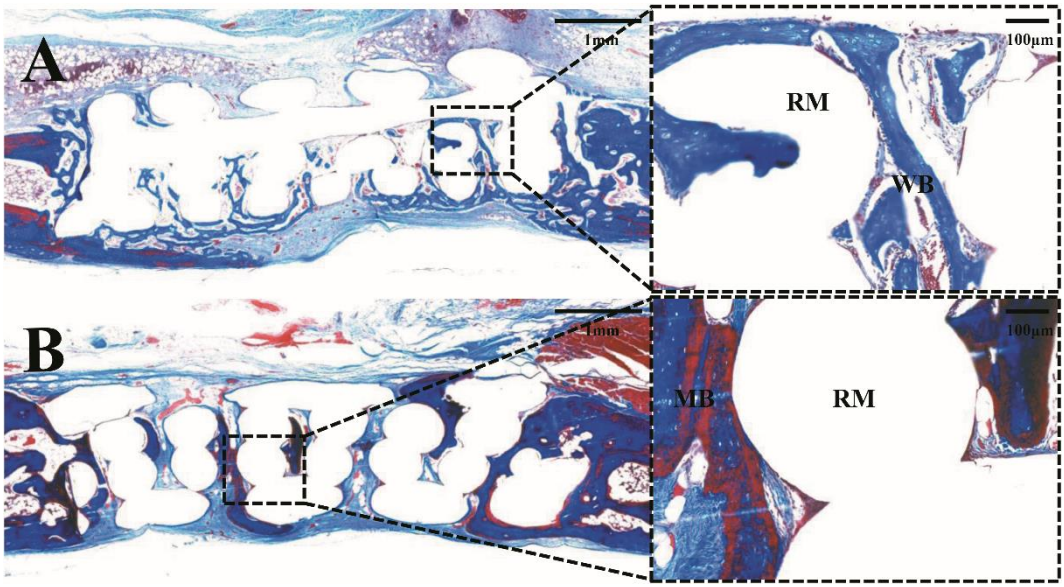

Figure 7. New bone formation around PCL/β-TCP scaffold (Masson Trichrome, bar=1mm) (A) PCL/β-TCP group at 2 weeks; Woven bone (WB) is well formed into the pore of the scaffold (RM). (B) PCL/β-TCP with membrane group at 8 weeks; Mature bone (MB) is directly contacting with the scaffold (RM).

Tables

Table 1. Total augmented volume and new bone volume measured with micro-CT grey value

		TAV	NBV
2 weeks *(n=5)*	Control	163.06 ± 32.46	16.41 ± 6.71
	PCL	187.87 ± 26.94	10.42 ± 4.44
	PCL/β-TCP	*217.06 ± 28.82	18.25 ± 5.45
	PCL/β-TCP + M	193.00 ± 23.50	15.01 ± 2.79
8 weeks *(n=5)*	Control	208.41 ± 37.11	27.22 ± 15.13
	PCL	190.28 ± 28.44	25.60 ± 21.06
	PCL/β-TCP	202.81 ± 35.68	29.26 ± 21.83
	PCL/β-TCP + M	216.25 ± 25.66	†35.34 ± 10.92

Values are presented as mean±standard deviation (mm^3).

* Statistically significant difference compared to the control group.

† Statistically significant difference compared to the corresponding groups at 2 weeks.

TAV=total augmented volume; NBV=new bone volume;

Table 2. Total augmented area, new bone area and residual material area (histomorphometric analysis**)**

		TAA	NBA	RMA
2 weeks *(n=5)*	Control	6.39 ± 1.50	1.52 ± 0.57	
	PCL	*13.96 ± 1.52	0.67 ± 0.59	6.30 ± 0.84
	PCL/β-TCP	*13.11 ± 1.33	0.86 ± 0.87	6.90 ± 0.70
	PCL/β-TCP + M	*14.31 ± 2.04	0.79 ± 0.75	7.26 ± 1.67
8 weeks *(n=5)*	Control	6.24 ± 1.71	2.63 ± 0.95	
	PCL	*14.93 ± 3.26	1.61 ± 1.03	6.83 ± 0.60
	PCL/β-TCP	*10.93 ± 1.84	*1.20 ± 0.62	5.24 ± 0.91
	PCL/β-TCP + M	*11.59 ± 0.79	†2.66 ± 0.91	4.61 ± 0.84

Values are presented as mean±standard deviation (mm^2).

* Statistically significant difference compared to the control group.

† Statistically significant difference compared to the corresponding groups at 2 weeks.

TAA=total augmented area; NBA=new bone area; RMA=residual material area.

국문요약

토끼 두개골 결손부에서 3D 프린팅된 베타 삼인산칼슘 첨가 폴리카프로락톤 스캐폴드를 이용한 골재생

<지도교수 **최 성 호**>

연세대학교 대학원 치의학과

배 형 철

3D 프린팅된 블록형 골이식재를 이용한 결손부 맞춤형 골재생이 개발되고 있다. 폴리카프로락톤은 이러한 기술의 3D 스캐폴드로 사용될 수 있는 생체적합성을 갖는 고분자 재료다. 이 연구의 목적은 3D 프린팅된 폴리카프로락톤 스캐폴드의 골형성능과 생체적합성을 평가하고, 폴리카프로락톤 스캐폴드에 베타 삼인산칼슘(β-tricalcium phosphate)을 첨가하는 것의 효과를 평가하는 것이다.

직경 8 mm, 높이 1.9 mm 크기로 3D 프린팅된 폴리카프로락톤 블록과 무게비 10%의 베타 삼인산칼슘을 첨가한 폴리카프로락톤 블록을 준비하였다. 네 개의 군을 i) 음성 대조군(대조군), ii) 폴리카프로락톤 블록을 적용한 군

(PCL 군), iii) 무게비 10%의 베타 삼인산칼슘을 첨가한 폴리카프로락톤 블록을 적용한 군(PCL/β-TCP 군), iv) PCL/β-TCP 군에 콜라겐 차단막까지 덮은 군 (PCL/β-TCP + M 군)으로 설정하였다. 토끼 두개골에 네 개의 원형 결손부(직경 8 mm)를 형성하고 네 개의 군을 각 결손부에 적용하였다. 실험에 사용된 토끼는 2주(*n=5)* 및 8주(*n=5*)에 안락사시켰으며, 방사선학적 및 조직학적 분석을 진행하였다.

방사선학적 분석에서 8주 후에 PCL/β-TCP + M 군이 신생골의 부피 측면에서 가장 높은 값을 보였으나 네 그룹 간에 유의미한 차이는 없었다. 조직계측학적 분석에서 나머지 세 군은 대조군에 비해 증강된 면적의 값이 유의미하게 높았다. PCL/β-TCP + M 군은 신생골 면적의 값이 가장 높았지만 대조군과 유의미한 차이는 없었다. 베타 삼인산칼슘이 첨가된 폴리카프로락톤 스캐폴드에서만 스캐폴드 내부 깊은 곳까지 신생골 형성이 관찰되었다.

폴리카프로락톤은 높은 부피안정성과 생체적합성을 보였다. 폴리카프로락톤에 베타 삼인산칼슘을 첨가하면 친수성과 골 전도성이 증가하는 것으로 보인다. 3D 프린팅된 폴리카프로락톤 재료의 추가적인 연구가 필요할 것으로 보인다.

핵심되는 말: 골재생, 베타 삼인산칼슘, 폴리카프로락톤, 3D 프린팅